Int. J. Non-Linear Mechanics, Vol. 27, No. 5, pp. 875–888, 1992
Printed in Great Britain.

0020–7462/92 $5.00 + .00
Pergamon Press Ltd

NORMAL MODES AND GLOBAL DYNAMICS OF A TWO-DEGREE-OF-FREEDOM NON-LINEAR SYSTEM—II. HIGH ENERGIES

A. F. VAKAKIS

Department of Mechanical and Industrial Engineering, University of Illinois at Urbana-Champaign, Urbana, IL 61801, U.S.A.

and

R. H. RAND

Department of Theoretical and Applied Mechanics, Cornell University, Ithaca, NY 14853, U.S.A.

(*Received* 23 *January* 1991; *in revised form* 3 *June* 1991)

Abstract—The high-energy global dynamics of an undamped, strongly non-linear, two-degree-of-freedom system are considered. As shown in an earlier work [A. F. Vakakis and R. H. Rand, *Int. J. Non-Linear Mech.* **27**, 861–874 (1992)], the oscillator under consideration contains "similar" non-linear normal modes and at certain values of its structural parameters a mode bifurcation is possible. For low energies, the mode bifurcation gives rise to a homoclinic orbit in the Poincaré map of the system. For high energies, large- and low-scale chaotic motions are detected, resulting from transverse intersections of the stable and unstable manifolds of an unstable antisymmetric normal mode, and from the breakdown of invariant KAM-tori. The creation of additional free subharmonic motions is studied by a subharmonic Melnikov analysis, and the stability of the subharmonic motions is examined by an averaging methodology. The main conclusion of this work is that the bifurcation of similar normal modes results in a class of large-scale free chaotic motions, which do not exist in the system before the bifurcation.

1. INTRODUCTION

In a previous work [1], the low-energy dynamics of a two degree-of-freedom (DOF) system with cubic stiffness non-linearities were examined. It was shown that the system possessed "similar" non-linear normal modes, i.e. free periodic motions during which all coordinates vibrated equiperiodically, reaching their extremum values at the same instant of time [2, 3]. Moreover, a Hamiltonian pitchfork bifurcation of normal modes existed for the system, during which an antisymmetric mode lost stability giving rise to a pair of bifurcating additional similar modes.

An interesting feature of the low-energy dynamics was the existence of a homoclinic orbit in the *Poincaré map* of the system, which resulted from the identification of the stable and unstable manifolds of the orbitally unstable antisymmetric mode [1]. This homoclinic orbit has a highly degenerate structure; as the energy of the motion is increased, transverse intersections of the stable and unstable manifolds are expected to occur, giving rise to complicated chaotic motions [4, 5].

Although analytical averaging techniques exist for studying the transverse intersections of stable and unstable manifolds of perturbed homoclinic orbits (homoclinic Melnikov theory [4, 5]), they cannot be applied to study the "breakdown" of the homoclinic orbit of the Hamiltonian system under consideration. This is because the homoclinic orbit encountered in this work occurs in the *slow (averaged) flow* of the dynamical system [1], and as a result, the associated homoclinic Melnikov functions become exponentially small as a certain perturbation parameter decreases [1, 4]. Certain recent works address this limitation of Melnikov analysis [6, 7], but no general theory dealing with this problem yet exists; thus, the only possible way for studying the breakdown of the homoclinic orbit that appears in the "slow flow" is by direct numerical integrations of the equations of motion of the system.

Due to the "non-integrability" [8] of the Hamiltonian system under consideration, an additional class of free subharmonic and chaotic motions is possible. These motions result

from the breakdown of the "rational" KAM-tori of the system [4, 8], and can be studied by both analytical and numerical techniques. Holmes and Marsden [9, 10] developed a perturbation method for studying the subharmonic motions generated from the breakdown of "resonant" tori in a system of weakly coupled pendula. An analogous calculation was performed in ref. [11], and the existence of an arbitrarily large number (but not of an infinity of) subharmonic motions was detected in a pendulum-spring system. The stability of the generated subharmonic motions was analytically examined in refs [11–13].

In this work, both analytical and numerical techniques are used to study the high-energy global dynamics of the two-DOF system first introduced in ref. [1]. In Section 2, numerical, high-energy Poincaré maps are shown and large- and low-scale free chaotic motions are detected. In Section 3, the free chaotic motions resulting from transverse homoclinic intersections of the stable and unstable manifolds of the antisymmetric mode of the system are numerically studied. In Section 4, the subharmonic Melnikov analysis of [9, 10] is implemented for proving the existence of a class of subharmonic free motions in the dynamics of the system. In Section 5, the stability of the identified subharmonic motions is analytically examined and in Section 6, a discussion of the findings of this work is given.

2. DYNAMICS FOR HIGH ENERGIES

The system under consideration appears in Fig. 1, and consists of two equal masses connected by three stiffnesses with cubic non-linearity. The differential equations of motion are given by

$$\ddot{x}_1 + x_1 + x_1^3 + K(x_1 - x_2)^3 = 0 \tag{1a}$$

$$\ddot{x}_2 - K(x_1 - x_2)^3 + x_2 + x_2^3 = 0. \tag{1b}$$

The oscillator is said to be in a "1–1 resonance" since its linearized eigenvalues are equal. Depending on the value of the coupling parameter K, the system can have either two of four similar normal modes [1]. For $K > 1/4$ ("strong coupling") there exist two orbitally stable modes: a symmetric one corresponding to $x_1 = x_2$, and an antisymmetric one corresponding to $x_1 = -x_2$. When $K < 1/4$ ("weak coupling"), the antisymmetric mode becomes orbitally unstable giving rise to two orbitally stable bifurcating modes. In ref. [1], the low-energy global dynamics of the system were investigated by means of Poincaré maps. These maps were constructed by "cutting" the dynamical flow on the three-dimensional isoenergetic manifold of the system by the two-dimensional surface $\{x_1 = 0\}$, and by recording the values of x_2 and $\dot{x}_2$ at the "cut" section corresponding to positive velocities $\dot{x}_1 > 0$ [1]. In Fig. 2(a), the Poincaré map of the system with $K = 0.1 < 1/4$ and total energy $h = 0.4$ is shown. It can be shown [1] that the low-energy global dynamics of the system can be approximately analyzed and predicted.

In this section it will be shown that when the energy of oscillation is increased, there exists complicated, random-like chaotic motions that cannot be predicted by any standard method of analysis. In order to study such complicated motions, numerical techniques must be implemented, and in fact, the Poincaré map will be the basic tool in the following investigations of the large amplitude motions of the system.

The differential equations of motion (1) were numerically integrated with a fourth-order Runge–Kutta algorithm, and Poincaré section were constructed. The coupling stiffness parameter, K, was assigned the value $K = 0.1 < 1/4$ (corresponding to four normal modes of free oscillation), and the resulting Poincaré maps corresponding to $h = 50$ and $h = 150$

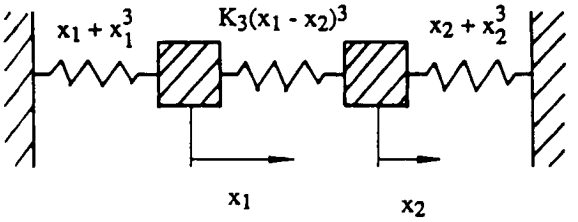

Fig. 1. The non-linear oscillator under consideration.

are presented in Fig. 2(a) and (b). Observe the global changes that occur in the Poincaré plot as the energy is increased:

— There are certain regions in the map where the orbits of the oscillator seem to wander erratically. These regions, the so-called "seas of stochasticity" [8], contain chaotic motions

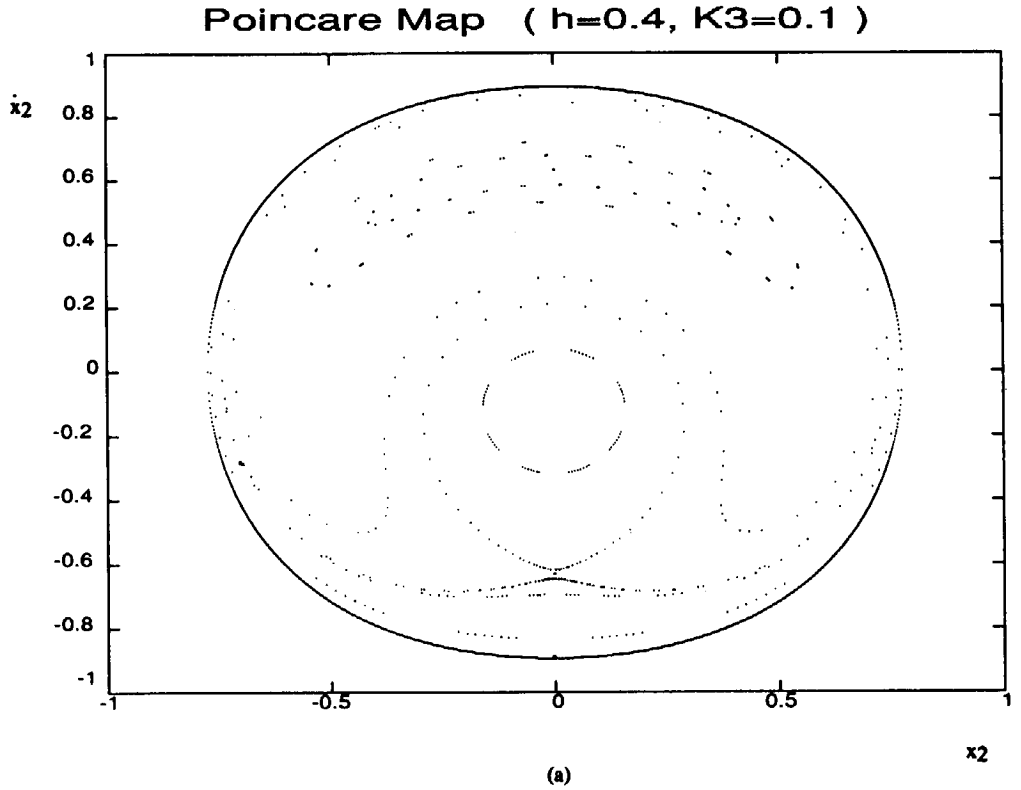

(a)

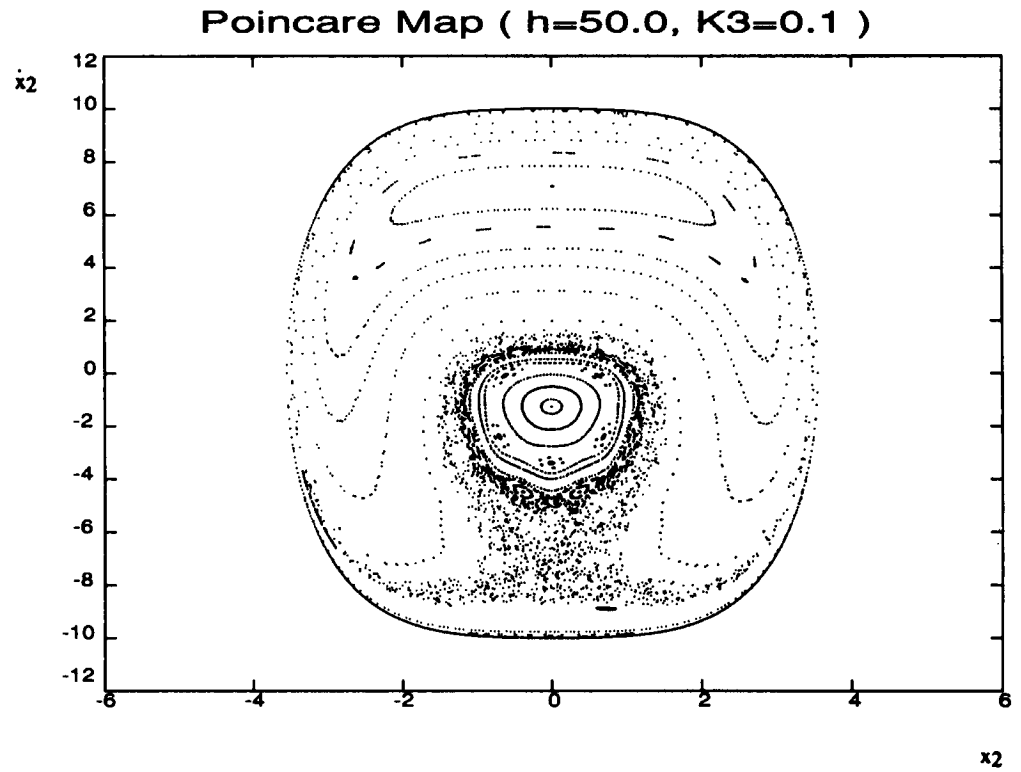

(b)

Fig. 2(a), (b).

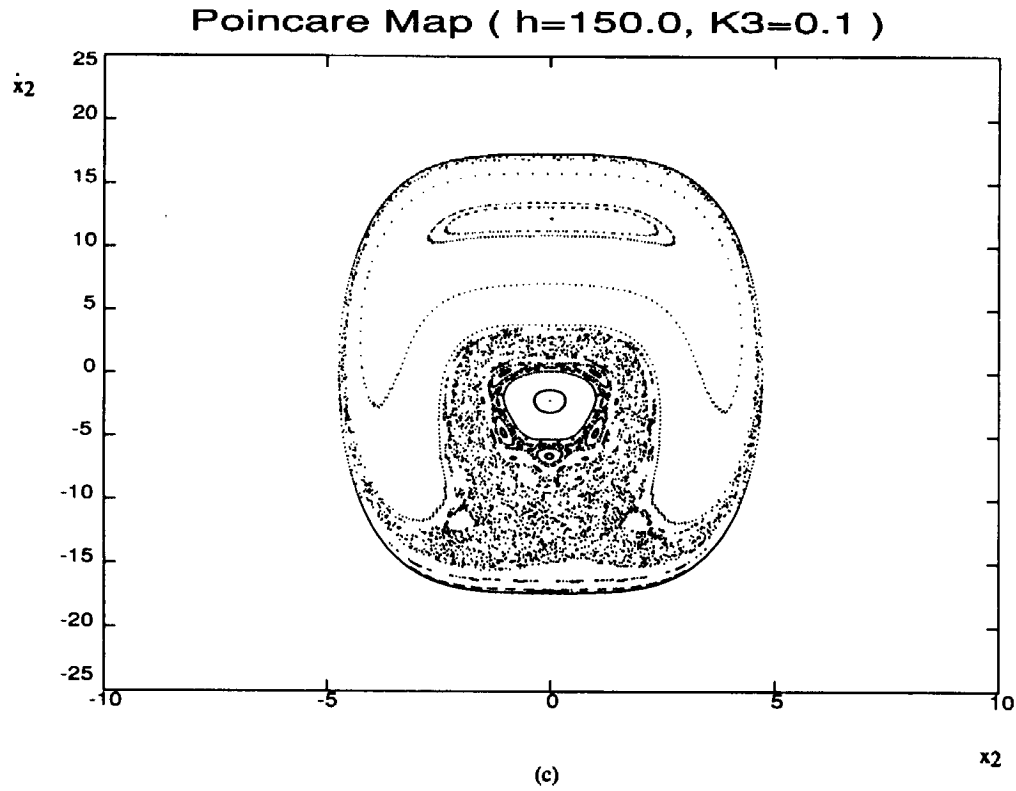

Fig. 2. Numerical Poincaré maps for a system with $K = 0.1 < 1/4$ and levels of energy: (a) $h = 0.4$, (b) $h = 50.0$, (c) $h = 150.0$.

of the Hamiltonian system, i.e. motions that have extreme sensitivity on initial conditions. In addition, one can detect a large "chaotic region" surrounding the (unstable) antisymmetric and the two (stable) bifurcated normal modes. In that region, large-scale chaotic motions occur.

— A careful examination of the plots indicates that some "islands in the stochastic sea" also exist; these consist of stable and unstable subharmonic orbits that are surrounded by small-scale chaotic motions.

— In Fig. 2(b), two closed curves appear to separate two subharmonic orbits of periods 6 (the outer) and 5 (the inner). Therefore, small-scale chaotic motions surrounding the two subharmonics are necessarily disconnected from each other, since they cannot cross the aforementioned closed curves. This confinement of chaotic motions is a unique feature of the two-DOF Hamiltonian oscillator and is not encountered in oscillators with more DOF (since in systems with n-DOF, $n \geq 3$, "Arnold diffusion" occurs [8]). The closed curves are the intersections with the cut-plane of "sufficiently irrational" KAM-tori, whereas the subharmonic orbits result from the breakdown of the rational ones [8].

— Numerical experiments show that the region of the phase space occupied by the stochastic sea increases with increasing energy. However, even for large energies regions exist in the phase plane where the free motion of the system is still predictable. For example, the symmetric mode is orbitally stable even for large energies and is surrounded by smooth closed curves that are intersections of tori with the cut section. So, although the chaotic region expands with increasing energy, it still remains confined to a certain region close to the antisymmetric and bifurcating modes, but away from the symmetric one.

In what follows, the large-scale chaotic motions (in the stochastic sea), and the small-scale ones (close to the subharmonic orbits), are examined separately.

3. TRANSVERSE HOMOCLINIC INTERSECTIONS OF INVARIANT MANIFOLDS

To study the chaotic motions that surround the antisymmetric and bifurcated modes, it is necessary to compute the stable and unstable invariant manifolds of the unstable mode.

A rigorous definition of the notion of "invariant manifold" can be found in refs [4, 5]. The manifolds are numerically computed by integrating the equations of motion on the energy surface, with initial conditions that are sufficiently close to those of the antisymmetric mode. Forward iterations of points close to the unstable mode give the unstable manifold, whereas backward iterations lead to the stable one.

In Fig. 3, the stable and unstable manifolds of the unstable antisymmetric mode are shown for the system with $K = 0.1$ and $h = 50.0$. Note the "violent windings" of the

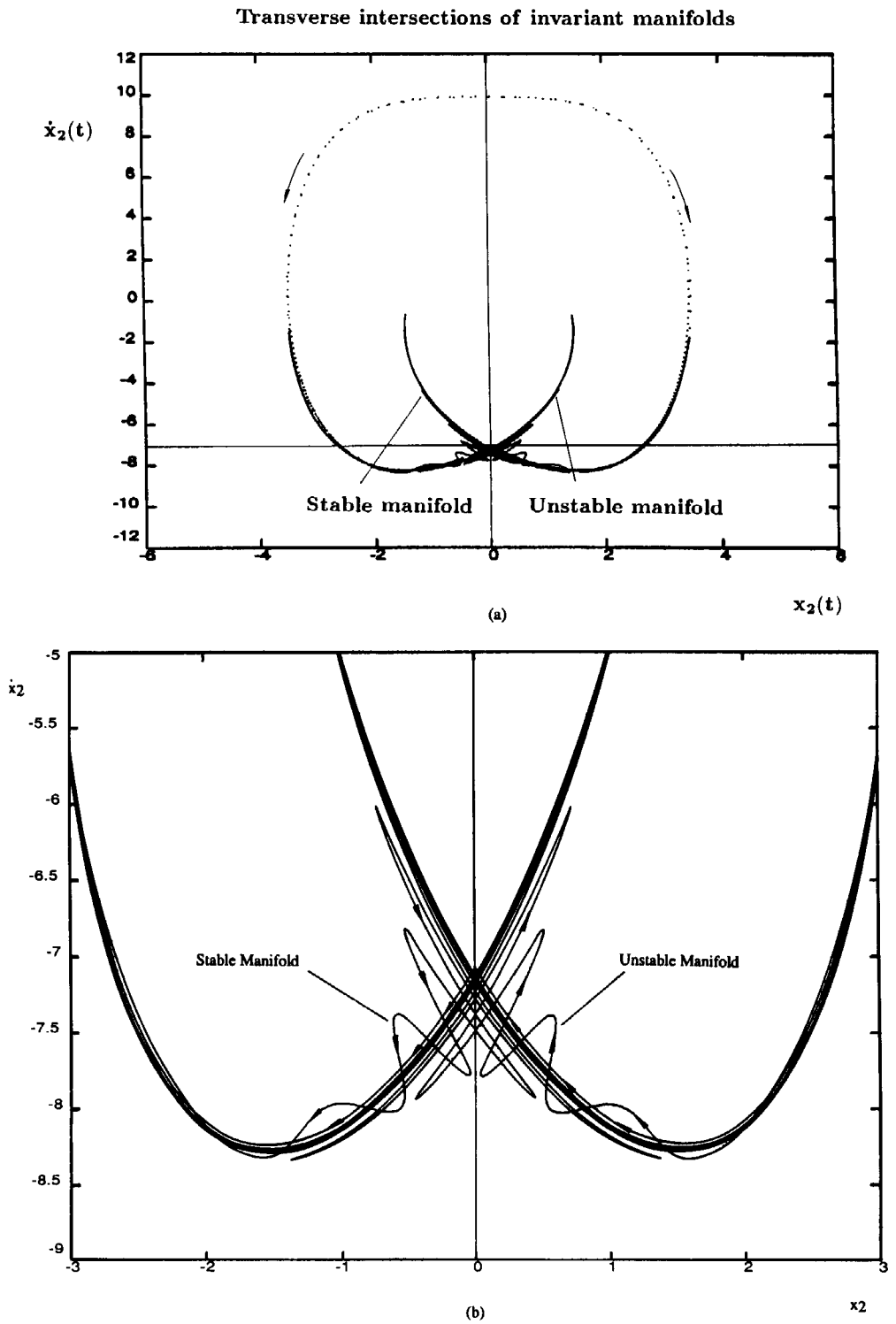

Fig. 3. Transverse intersections of stable and unstable manifolds of the antisymmetric mode for $K = 0.1$ and $h = 50.0$: (a) global Poincaré map, (b) close to the unstable antisymmetric mode.

manifolds as they approach the unstable mode. It can be proven that an infinite number of these "windings" exists as the manifolds accumulate on themselves ("lambda–lemma" [4]). An infinity of transverse intersections of the two manifolds then occurs forming an infinity of "Smale horseshoes". This has interesting implications in the dynamics of the Poincaré map. In fact, using the Smale–Birkhoff homoclinic theorem [4, 5], it can be shown that the Poincaré map contains a countable infinity of periodic orbits, an uncountable infinity of non-periodic orbits, and dense orbits. Thus, the dynamics of the map in the vicinity of the unstable mode has sensitive dependence on initial conditions and is virtually unpredictable. Note that this numerical demonstration of the existence of "homoclinic tangles" shows that transient chaos occurs in the map, but it does not imply the existence of a "strange attractor". Such attractors are only realizable in dissipative dynamical systems, and thus cannot be found in the dynamics of this Hamiltonian oscillator. No more details will be provided about these chaotic motions at this point, since a complete analysis of "horseshoe" maps can be found elsewhere [5].

An interesting observation is that this type of large-scale global chaos occurs only if the antisymmetric mode is orbitally unstable, since only then do one-dimensional invariant manifolds exist. For values of the coupling stiffness parameter, K greater than 1/4, no such motions can occur, since then the antisymmetric mode is orbitally stable and no bifurcating modes exist. (However, as shown in the next section, small-scale local chaotic motions are encountered in that case.)

In certain cases, homoclinic Melnikov functions can be used to analytically prove the existence of the aforementioned transverse intersections. Unfortunately, one cannot implement this kind of analysis in the present case, since the resulting Melnikov functions become exponentially small as the non-linearity decreases. (This is because, for low energies, the homoclinic orbit appears in the *averaged* Hamiltonian equations—for a discussion see refs [1, 4].) However, subharmonic Melnikov analysis can be used to prove the existence of subharmonic orbits in the Poincaré map.

4. SUBHARMONIC ORBITS—MELNIKOV ANALYSIS

Small-scale chaotic motions in the vicinity of the subharmonic orbits result from the destruction of the invariant tori of the Hamiltonian system, and are local in nature. Moreover, they occur irrespective of the pitchfork bifurcation of normal modes (occurring at $K = 1/4$); this is in contrast to the large-scale chaotic motions encountered in the previous section that occur only after the bifurcation of normal modes, i.e. only for $K < 1/4$. In what follows, a Melnikov-type analysis is implemented to study the generation of subharmonic orbits.

In this section, the perturbation methods developed by Holmes and Marsden [9, 10] will be implemented to prove the existence of arbitrarily many subharmonic orbits in the neighborhood of an orbit of the two-DOF, 1–1 resonant, Hamiltonian oscillator with cubic non-linearity. In refs [9, 10], this methodology was first applied to prove the non-existence of analytic second integrals of motion of a certain type, and to study the way in which resonant tori break-up between KAM irrational preserved tori, for a pair of weakly coupled pendula.

In order to apply the perturbation methodology of this section, it is necessary to assume that the coupling stiffness K in equations (1) is weak; however, no such assumption is needed for the end stiffnesses. The differential equations of motion are then of the form

$$\ddot{x}_1 + x_1 + x_1^3 + \varepsilon K(x_1 - x_2)^3 = 0 \tag{2a}$$

$$\ddot{x}_2 - \varepsilon K(x_1 - x_2)^3 + x_2^3 + x_2 = 0 \tag{2b}$$

where ε is a parameter of perturbation order, i.e. $|\varepsilon| \ll 1$. When $\varepsilon = 0$, the system degenerates into the following system of two (strongly) non-linear Hamiltonian oscillators:

$$\ddot{x}_1 + x_1 + x_1^3 = 0 \quad \text{("uncoupled oscillator 1")} \tag{3a}$$

$$\ddot{x}_2 + x_2 + x_2^3 = 0 \quad \text{("uncoupled oscillator 2").} \tag{3b}$$

Integrating by quadratures, one can obtain analytic solutions for the generalized coordin-

ates q_i and generalized momenta p_i [14] of the uncoupled Hamiltonian oscillators:

$$q_i = x_i(t) = X_i \operatorname{cn}([1 + X_i^2]^{1/2} t, k_i), \qquad k_i^2 = \frac{X_i^2}{2(1 + X_i^2)}, \quad i = 1, 2 \tag{4}$$

where the following set of initial conditions was assumed:

$$q_i = X_i, \qquad q_i(0) = 0, \quad i = 1, 2. \tag{5}$$

In the above expression, $\operatorname{cn}(\cdot, \cdot)$ is the elliptic cosine, and k_i is its modulus [15].

Assuming that the energy of the "uncoupled oscillator i" is equal to h_i $(i = 1, 2)$, its amplitude of oscillation X_i can be related to h_i by

$$X_i^2 = -1 + (1 + 4h_i)^{1/2}, \quad h_i > 0, \quad i = 1, 2. \tag{6}$$

Combining expressions (4) and (6), one can express the oscillations of the two unperturbed systems, in terms of their energies, as follows:

$$q_i(t) = [(H_i^{1/2} - 1)]^{1/2} \operatorname{cn}(H_i^{1/4} t, k_i)$$

$$k_i^2 = \frac{H_i^{1/2} - 1}{2H_i^{1/2}}, \quad i = 1, 2 \tag{7}$$

where the notation, $H_i \equiv (1 + 4h_i)$, was used. The generalized momenta of the uncoupled system result by direct differentiation with respect to time of expressions (7):

$$p_i(t) = \dot{q}_i(t) = -H_i^{1/4}(H_i^{1/2} - 1)^{1/2} \operatorname{sn}(H_i^{1/4} t, k_i) \operatorname{dn}(H_i^{1/4} t, k_i), \quad i = 1, 2 \tag{8}$$

where $\operatorname{sn}(\cdot, \cdot)$, $\operatorname{dn}(\cdot, \cdot)$ are elliptic functions [15].

Each of the uncoupled oscillators has a phase plane consisting of closed periodic orbits. Consider the flow of the coupled system in the neighborhood of the elliptic periodic orbit $\mathbf{p} = (0, p_2(t))$, $\mathbf{q} = (0, q_2(t))$, and for a fixed total energy h. Under certain conditions [11] (that are satisfied in the present case), it is possible to reduce the four-dimensional flow of the Hamiltonian oscillator (2) to the following form [9–11]:

$$\frac{\mathrm{d}q_1}{\mathrm{d}\theta_2} = -\frac{\partial L^0}{\partial p_1} - \varepsilon \frac{\partial L^1}{\partial p_1} + O(\varepsilon^2) \tag{9a}$$

$$\frac{\mathrm{d}q_1}{\mathrm{d}\theta_2} = \frac{\partial L^0}{\partial q_1} + \varepsilon \frac{\partial L^1}{\partial q_1} + O(\varepsilon^2) \tag{9b}$$

where

$$L^0(q_1, p_1; h) = F_2^{-1}[h - F_1(q_1, p_1)]$$

$$L^1(q_1, p_1, \theta_2; h) = -H^1[q_1, p_1, \theta_2; L^0(q_1, p_1; h)]/\Omega(L^0[q_1, p_1; h])$$

$$\Omega(I_2) = \mathrm{d}F_2(I_2)/\mathrm{d}I_2$$

and

$$F_i(p_i, q_i) = \frac{p_i^2}{2} + \frac{q_i^2}{2} + \frac{q_i^4}{2}, \quad i = 1, 2$$

$$H^1(\mathbf{p}, \mathbf{q}) = \frac{(q_1 - q_2)^4}{2}.$$

In the above expressions, the notation of ref. [11] was used; $F_i(p_i, q_i)$ is the Hamiltonian of the uncoupled oscillator i, and $H^1(\mathbf{p}, \mathbf{q})$ is the part of the Hamiltonian corresponding to the coupling stiffness of order ε. The quantities (I_2, θ_2) are the action-angle variables of the uncoupled oscillator 2 [14], and result from the original generalized variables (q_2, p_2) by means of a canonical symplectic transformation of coordinates. Note that the expression for L^0 results from the "symbolic inversion" of the quantity F_2. For a rigorous derivation of expressions (9), the interested reader is referred to refs [9, 10].

The "reduced" system (9) is in the form of a periodically perturbed planar oscillator. When $\varepsilon = 0$ the system is Hamiltonian with Hamiltonian function L^0, and "time-like" variable θ_2. For $\varepsilon \neq 0$, the Hamiltonian system is perturbed by "time-dependent" terms (this happens because the term L^1 has explicit periodic dependence on the time-like, angle

variable θ_2 which is modulo 2π). Thus, one can apply the Melnikov theory for subharmonic orbits [4] to the study of the reduced system. To do this, one must consider the unperturbed reduced phase space (q_1, p_1, θ_2) corresponding to $\varepsilon = 0$ in equations (9); one then can find a countable infinity of resonant tori for the unperturbed flow. These tori are direct products of the periodic orbits of the two single DOF "uncoupled oscillators 1 and 2", and in order for a torus to be resonant, it is necessary that the periods T_1 and T_2 of the uncoupled oscillators 1 and 2 satisfy the relation:

$$T_1 = \frac{mT_2}{n} \quad \text{(resonant torus for the uncoupled system with } \varepsilon = 0) \tag{10}$$

or for the specific system under consideration

$$\frac{nK(k_1)}{H_1^{1/4}} = \frac{mK(k_2)}{H_2^{1/4}} \quad \text{(resonance condition)} \tag{11}$$

where m and n are relatively prime positive integers.

In writing equation (11), the actual expressions for the periods of oscillation of the motions (7) were used, and $K(\cdot)$ is the complete elliptic integral of the first kind. In the Appendix it is shown that, for a given level of total energy h, a torus satisfying the resonance condition (11) exists only for a limited range of values for m and n. For example, for $h = 1$, equation (11) is satisfied only when the ratio m/n is in the range,

$$0.72411 \leq m/n \leq 1.38100 \quad (h = 1). \tag{12}$$

Hence, only a restricted class of resonant tori will be considered. It is the perturbations of these tori (when coupling is present) that will be examined in the following. Considering the unperturbed, reduced equations (9) (with $\varepsilon = 0$), and assuming that the resonance conditions (10) and (11) are satisfied, the motion on a resonant torus of the unperturbed reduced phase space corresponding to initial conditions $(q_1(0), p_1(0), \theta_0)$ and unperturbed energy level h_1 is denoted by

$$[q_1(\theta), p_1(\theta), \theta + \theta_0] \quad \text{(resonant torus of the unperturbed reduced phase space)} \tag{13}$$

where θ is a variable parametrizing the motion on the resonant torus. Since the resonance conditions (10) and (11) are satisfied, a point in the unperturbed phase space corresponding to $\theta = \theta_0$ coincides with its image at $\theta = \theta_0 + 2\pi m$. When the "perturbed", reduced flow is considered ($\varepsilon \neq 0$ in equation (9)), the distance between the initial point at θ_0 and its image at $\theta_0 + 2\pi m$ will not be zero; in fact, to the first order of accuracy this distance can be computed as [4]

$$\mathrm{d}(\theta_0) = \varepsilon \frac{M(\theta_0; m, n, h)}{\| X_F(0) \|} + O(\varepsilon^2) \tag{14}$$

where $\| X_F(0) \|$ is a normalization scalar factor [4], and $M(\theta_0, m, n, h)$ is the subharmonic-Melnikov function defined by

$$M(\theta_0, m, n, h) = \int_0^{2\pi m} \{L^0, L^1\}_{[q_1(\theta_2 - \theta_0), p_1(\theta_2 - \theta_0), \theta_2, h]} \mathrm{d}\theta_2 \tag{15}$$

where, $\{\cdot, \cdot\}$ is the Poisson bracket [4]. A basic theorem then states that, when the distance equation (14) between the image points in the perturbed flow vanishes, a subharmonic orbit results in the coupled system. Thus, by studying the zeros of the Melnikov function (15), one can analytically predict the generation of subharmonic orbits in the global dynamics of the coupled system.

As pointed out in equation (11), this Melnikov technique proves the existence of only a finite number of periodic orbits in the vicinity of an unperturbed resonant torus. This is because as the integers $m, n \to \infty$, one must let $\varepsilon \to 0$, in order to guarantee that the term $\varepsilon M / \| X_F \|$ dominates over the $O(\varepsilon^2)$ terms. Thus, one cannot prove the existence of infinitely many periodic orbits, and as a result, one cannot rigorously prove the non-integrability of the Hamiltonian system under consideration.

The Melnikov function (15) can be written in the following form that is convenient for numerical computations [9–11]:

$$M(t_0, m, n, h) = \frac{T_2}{2\pi} \int_{-mT_2/2}^{mT_2/2} \left(\frac{\partial F_1}{\partial q_1} \frac{\partial H^1}{\partial p_1} - \frac{\partial F_1}{\partial p_1} \frac{\partial H^1}{\partial q_1} \right)_{[q^1(t), p^1(t), q^2(t+t_0), p^2(t+t_0), h]} \mathrm{d}t \tag{16}$$

or for the system under consideration

$$M(t_0, m, n, h) = \frac{T_2}{2\pi} \int_{-mT_2/2}^{mT_2/2} - p_1(t)[q_1(t) - q_2(t + t_0)]^3 \, \mathrm{d}t \tag{17}$$

where $T_2 = K(k_1)/H_1^{1/4}$ is the period of oscillation of the unperturbed motion of "uncoupled oscillator 2" on the fixed energy level h, $q_i(t)$, $p_i(t)$ are the unperturbed oscillations given by expressions (4) and (8), and F_1, H^1 are the Hamiltonian functions defined earlier.

From the aforementioned discussion, a necessary condition for the existence of subharmonic motions for the perturbed system is that the equation,

$$M(t_0, m, n, h) = 0 \tag{18}$$

has a finite number of simple zeros. The study of the zeros of the Melnikov function is tedious and here, only the final results will be given. For a detailed analysis the reader should consult [16] where all the necessary calculations are provided. It can be proven that, for any given integers m and n in the permissible range defined in the Appendix, the Melnikov function (17) has $2m$ zeros corresponding to $t_0 = kT_2/2$, where the integer k is defined by the relation $kn \bmod 2m = 0, 1, \ldots, 2m - 1$, in the interval $0 \leq kn/2m < 1$. In addition, a lengthy calculation shows that these zeros are simple [16], i.e.

$$\left[\frac{\mathrm{d}M(t_0, m, n, h)}{\mathrm{d}t_0} \right]_{t_0 = kT_2/2} \neq 0. \tag{19}$$

Thus, the analytic proof of the existence of subharmonic orbits in the dynamics of the two-DOF system under consideration is completed. Moreover, it can be verified [16] that the outlined subharmonic Melnikov analysis fails as $n, m \to \infty$. In that case

$$\lim_{m,n \to \infty} \left\{ \left[\frac{\mathrm{d}M(t_0, m, n, h)}{\mathrm{d}t_0} \right]_{t_0 = kT_2/2} \right\} = 0 \tag{20}$$

and the conclusion is that one cannot prove the existence of subharmonic orbits of all resonant tori in any neighborhood of an elliptic orbit (this can only be proved for finite values of m and n). An analogous calculation was first performed in a pendulum–spring system [11].

As an example, consider the energy level $h = 1$, and a resonant torus corresponding to $m/n = 11/13$. The value of the ratio m/n is within the range (12) specified by the inequalities of the Appendix; hence, equation (A1) of the Appendix has a unique root for h_1, which can be numerically computed as $h_1 = 0.776$. This gives a value for h_2 equal to $h_2 = h - h_1 = 0.224$. At these energy levels of the uncoupled oscillators 1, 2, a resonant torus exists. There are $2m = 22$ simple zeros of the Melnikov function, and thus one concludes that at the energy level $h = 1$, a resonant torus breaks into two distinct, 22π-periodic orbits.

For the energy level $h = 50$, the perturbation analysis predicts the break or resonant tori with values of m/n in the range [0.3087, 3.2395] (see Appendix). Thus, for $m = 5$, $5 > n > 1$, the theory predicts that a resonant torus breaks into two distinct, 10π-periodic orbits. As shown in the next section, one of these orbits is stable, whereas the other is unstable. In Fig. 2(b), such a stable subharmonic orbit corresponding to $m = 5$ can be seen at the energy level $h = 50$.

5. PHASE-PLANE REPRESENTATION OF THE SUBHARMONIC ORBITS

The stability of the subharmonic orbits that result from the destruction of the rational tori will be examined by studying their phase-plane representation. To do this, a similar methodology with that presented in [11–13] will be applied. Consider at this point, the

reduced system of equations (9):

$$\frac{dq_1}{d\theta_2} = -\frac{\partial L^0}{\partial p_1} - \varepsilon\frac{\partial L^1}{\partial p_1} + O(\varepsilon^2) \tag{9a}$$

$$\frac{dq_1}{d\theta_2} = \frac{\partial L^0}{\partial q_1} + \varepsilon\frac{\partial L^1}{\partial q_1} + O(\varepsilon^2) \tag{9b}$$

where θ_2 is the time-like variable; as mentioned earlier, for $\varepsilon = 0$, the unperturbed system is Hamiltonian with Hamiltonian function L^0. Introducing action-angle variables [14] for the "uncoupled oscillator 1",

$$(p_1, q_1) \to (I_1, \theta_1)$$

one can symbolically write

$$I_1 = I_1(p_1, q_1), \qquad p_1 = p_1(I_1, \theta_1)$$
$$\theta_1 = \theta_1(p_1, q_1), \qquad q_1 = q_1(I_1, \theta_1). \tag{21}$$

The reduced set of equations (9) can be now symbolically transformed into the new variables I_1 and θ_1 [11]:

$$\frac{dI_1}{d\theta_2} = \varepsilon\frac{\partial \hat{L}^1(I_1, \theta_1, \theta_2)}{\partial \theta_1} + O(\varepsilon^2) \tag{22a}$$

$$\frac{d\theta_1}{d\theta_2} = -\omega(I_1) - \varepsilon\frac{\partial \hat{L}^1(I_1, \theta_1, \theta_2)}{\partial I_1} + O(\varepsilon^2) \tag{22b}$$

where $\omega(I_1) = d\hat{L}^0(I_1)/dI_1$, and $L^0(p_1, q_1, h) \equiv \hat{L}^0(I_1, h)$, $L^1(q_1, p_1, \theta_2) \equiv \hat{L}^1(I_1, \theta_1, \theta_2)$, are symbolic expressions in terms of the new variables I_1 and θ_1. Note that there is no explicit dependence of $\hat{L}^0$ on θ_1, since (I_1, θ_1) are the action-angle variables of the uncoupled oscillator 1.

Consider now an unperturbed orbit on the resonant torus with $nT_1 = mT_2$, by setting $\varepsilon = 0$ in equations (9), and integrating

$$I_1 = \bar{I}_1 \tag{23a}$$

$$\theta_1 = -\omega(I_1)\theta_2 = -\frac{n}{m}\theta_2. \tag{23b}$$

In the above expressions, $\bar{I}_1$ denotes the fixed value of the action variable on the unperturbed orbit. At this point, small perturbations of the following form are introduced:

$$I_1 = \bar{I}_1 + \varepsilon^{1/2}K \tag{24a}$$

$$\theta_1 = -\frac{n}{m}\theta_2 + \varepsilon^{1/2}\psi. \tag{24b}$$

The quantities K and ψ represent the perturbing terms. Note that the perturbations are assumed to be of $O(\varepsilon^{1/2})$ [11, 12]; this is necessary for a correct balancing of the terms in the perturbation analysis that follows.

Substituting expressions (24) into the reduced system (9), and after some manipulations, one obtains the following set of differential equations that must be satisfied by the quantities K and ψ:

$$\frac{dK}{d\theta_2} = \varepsilon^{1/2}\frac{\partial \hat{L}^1\left(\bar{I}_1, -\frac{n\theta_2}{m} + \psi, \theta_2\right)}{\partial \theta_1} + \varepsilon\frac{\partial \hat{L}^1\left(\bar{I}_1, -\frac{n\theta_2}{m} + \psi, \theta_2\right)}{\partial I_1}K + O(\varepsilon^{3/2})$$

$$\frac{d\psi}{d\theta_2} = -\varepsilon^{1/2}\frac{d\omega(\bar{I}_1)}{dI_1}K - \varepsilon\left[\frac{\partial^2 \hat{L}^1\left(\bar{I}_1, -\frac{n\theta_2}{m} + \psi, \theta_2\right)}{\partial I_1^2} + \frac{d^2\omega(\bar{I}_1)}{dI_1^2}\frac{K^2}{2}\right] + O(\varepsilon^{3/2}). \tag{25}$$

Following the methodology outlined in [11, 12], one applies the averaging theorem for $\varepsilon^{1/2}$

sufficiently small, in order to remove the explicit dependence of (25) from the "fast variable" θ_2. The resulting averaged equations are

$$\frac{d\bar{K}}{d\theta_2} = \frac{\varepsilon^{1/2}}{2\pi n} M\left[\frac{\bar{\psi}}{\omega(\bar{I}_1)}, m, n, h\right] \tag{26a}$$

$$\frac{d\bar{\psi}}{d\theta_2} = -\varepsilon^{1/2} \frac{d\omega(\bar{I}_1)}{dI_1} \bar{K}. \tag{26b}$$

In the above averaged equations, the quantity M is the subharmonic Melnikov function encountered in the previous section (defined by equations (15)–(17)), with the argument t_0 replaced by the new variable $\bar{\psi}/\omega(\bar{I}_1)$. Also note that the new variables $\bar{K}$ and $\bar{\psi}$ were used in the averaged equations, in order to distinguish them from expressions (25).

Under the averaging theorem, the hyperbolic and elliptic fixed points of equations (26) correspond to small periodic motions of the variations K and ψ, and therefore to subharmonics of order (m/n) for the reduced system (9). However, a necessary and sufficient condition for the existence of such fixed points for equations (26) is that the subharmonic Melnikov function has simple zeros, and that $\omega(\bar{I}_1) \neq 0$.

For the specific two-DOF oscillator under consideration, the Melnikov function was computed earlier, and the only unknown quantity in the averaged equations is the derivative $d\omega(\bar{I}_1)/dI_1$. This computation was performed in ref. [16], and the final result is as follows:

$$\frac{d\omega(\bar{I}_1)}{dI_1} = -\frac{\pi[E(k_1)(1-2k_1^2) - K(k_1)(1-k_1^2)](1-2k_1^2)}{8K^3(k_1)k_1^2(1-k_1^2)} \tag{27}$$

where $K(\cdot)$ and $E(\cdot)$ are the complete elliptic integrals of the first and second kind, respectively, and k_1 is the elliptic modulus. This is related to the energy h_1 of the uncoupled oscillator 1, h_1, by expression (7)

$$h_1 = \frac{1}{4}\left[\frac{1}{(1-2k_1^2)^2} - 1\right]. \tag{28}$$

Thus, the right-hand sides of the averaged, Hamiltonian equations (26) are explicitly known. In the previous section it was proved that for an (m/n) resonant torus, the associated Melnikov function has $2m$ simple zeros. Considering now expression (7), note that

$$1 - 2k_1^2 > 0 \quad \text{for } h_1 > 0, \qquad \text{and} \qquad \lim_{h_1 \to \infty} k_1^2 = 1/2. \tag{29}$$

Thus, the factor $[1 - 2k_1^2]$ in the numerator of expression (27) is always positive for positive values of h_1. Moreover, from simple properties of complete elliptic integrals [15], it can be proved that the following inequalities hold:

$$\begin{aligned} E(k_1)(1-2k_1^2) - K(k_1)(1-k_1^2) &< E(k_1)(1-k_1^2) - K(k_1)(1-k_1^2) \\ &< [E(k_1) - K(k_1)](1-k_1^2) < 0. \end{aligned} \tag{30}$$

In deriving the aforementioned relations, use was made of the known inequality [15] $E(k) - K(k) < 0$. Combining relations (29) and (30), one obtains the final basic result:

$$\frac{d\omega(\bar{I}_1)}{dI_1} > 0. \tag{31}$$

Considering now the averaged equations (26), and taking into account inequality (31), one can prove that for positive (negative) values of $\bar{K}$, the variable $\bar{\psi}$ is a decreasing (increasing) function of the time-like variable θ_2

$$\operatorname{sgn}\left(\frac{d\bar{\psi}}{d\theta_2}\right) = -\operatorname{sgn}(\bar{K}). \tag{32}$$

From the aforementioned discussion, one can draw a schematic representation of the phase plane of the averaged equations (26). From equation (32) it is concluded that the phase plane is rotating counterclockwise with increasing θ_2, and that its fixed points correspond to the zeros of the Melnikov function M.

Half of the fixed points are elliptic (and thus orbitally stable), whereas the remaining ones are hyperbolic (orbitally unstable). The elliptic and hyperbolic points alternate and the averaging theorem does not guarantee that the families of heteroclinic orbits connecting the hyperbolic points are preserved as smooth manifolds. In fact, the stable and unstable manifolds of the hyperbolic points intersect transversely, leading to chaotic motions (that are confined between preserved sufficiently irrational KAM-tori). Unfortunately, one cannot analytically prove the existence of these transverse intersections by a Melnikov-type analysis, since the resulting Melnikov functions become exponentially small as the perturbation parameter ε tends to zero.

The elliptic points are surrounded by closed curves; these correspond to the "islands" observed in the numerical Poincaré plots. To this order of approximation, only "primary islands" [8] are observed. However, by introducing new canonical transformations and rescaling, one could predict "secondary islands," within the primary islands. A disadvantage of this averaging analysis is that it cannot model the ergodic motion (sea of stochasticity) observed in the numerical Poincaré plots. This is because the averaged equations will always be in Hamiltonian form and, as such, will always possess a first integral of motion. Thus, irrespective of the order of approximation, all curves in the averaged phase planes correspond to a fixed value of the first integral and no chaotic motions are predicted.

6. DISCUSSION

The high-energy free oscillations of a strongly non-linear, discrete, Hamiltonian oscillator with cubic non-linearity were examined. It was found that when the energy of oscillation is increased, a sea of stochasticity appears in the Poincaré maps of the system, indicating the existence of random-like, highly unpredictable, chaotic motions. Additional stochastic layers occur in the vicinity of free subharmonic motions, and are due to the non-integrability of the Hamiltonian system (i.e. to the non-existence of a second analytic integral of motion, independent from the energy).

Large- and small-scale chaotic motions are identified in the high-energy Poincaré maps. The large-scale chaotic motions are a direct result of the pitchfork bifurcation of the normal modes of the system: they appear only after the mode bifurcation (when the antisymmetric mode is orbitally unstable), and they result from the transverse intersections of the stable and unstable manifolds of the antisymmetric mode (i.e. from the "destruction" of the homoclinic orbit seen in the low-energy Poincaré map). Local, small-scale chaotic motions result from the breakdown of "rational invariant tori" of the system. They appear close to subharmonic orbits of the oscillator and are confined in specific regions of the map.

Therefore, a necessary condition for large-scale chaos in this system is the orbital instability of the antisymmetric mode (since only then can large-scale transverse intersections of invariant manifolds occur). As a result, the bifurcations of normal modes appear to increase the complexity of the high-energy, free motions of the oscillator and in fact, one can state that the system after the bifurcation of the normal modes becomes "more chaotic" than the one before the mode bifurcation.

The subharmonic orbits generated from the destruction of the rational invariant tori of the oscillation were analytically examined by constructing suitable subharmonic Melnikov functions. In principle, a similar Melnikov-type perturbation analysis could be used to analytically prove the existence of transverse intersections between the stable and unstable manifolds of the antisymmetric mode. However, the resulting homoclinic Melnikov function becomes exponentially small as the perturbation parameter tends to zero, and this causes a failure of the perturbation scheme.

Acknowledgements—The first author wishes to thank Professor Thomas Caughey and Professor Steven Wiggins of the California Institute of Technology for informative and helpful discussions on several aspects of this work.

REFERENCES

1. A. F. Vakakis and R. H. Rand, Normal modes and global dynamics of a two-degree-of-freedom nonlinear system—I. Low energies. *Int. J. Non-Linear Mech.* **27**, 861–874 (1992).

2. R. Rosenberg, The normal modes of nonlinear n-DOF systems. *J. appl. Mech.* **30**, 7–14 (1962).
3. R. Rosenberg, On nonlinear vibrations of systems with many DOF. *Adv. appl. Mech.* **9**, 155–242 (1966).
4. J. Guckenheimer and P. Holmes, *Non-linear Oscillations, Dynamical Systems, and Bifurcations of Vector Fields.* Springer, Berlin (1984).
5. S. Wiggins, *Global Bifurcations and Chaos: Analytical Methods.* Springer, Berlin (1989).
6. P. Holmes, J. Marsden and J. Scheurle, Exponentially small splittings of separatrices with applications to KAM theory and degenerate bifurcations. *Contemporary Mathematics* **81**, 213–244 (1988).
7. A. Neishtadt, The separation of motions in systems with rapidly rotating phase. *PMM* **48**, 133–139 (1984).
8. A. Lichtenberg and M. Lieberman, *Regular and Stochastic Motions.* Springer, Berlin (1983).
9. P. Holmes and J. Marsden, Horseshoes in perturbations of Hamiltonian systems with two DOF. *Commun. Math. Phys.* **82**, 523–544 (1982).
10. P. Holmes and J. Marsden, Melnikov's method and Arnold diffusion for perturbations of integrable Hamiltonian systems. *J. Math. Phys.* **23**, 669–675 (1982).
11. P. Veerman and P. Holmes, The existence of arbitrarily many distinct periodic orbits in a two DOF Hamiltonian system. *Physica* **14D**, 177–192 (1985).
12. P. Veerman and P. Holmes, Resonance bands in a two-DOF Hamiltonian system. *Physica* **20D**, 413–422 (1986).
13. B. Greenspan and P. Holmes, Homoclinic orbits, subharmonics and global bifurcations in forced oscillators, in *Nonlinear Dynamics and Turbulence.* Pitman, New York (1983).
14. I. Persival and D. Richards, *Introduction to Dynamics.* Cambridge University Press, New York (1982).
15. P. Byrd and D. Friedman, *Handbook of Elliptic Integrals for Engineers and Physicists.* Springer, Berlin (1954).
16. A. Vakakis, Analysis and identification of linear and non-linear normal modes in vibrating systems. PhD thesis, California Institute of Technology, California.

APPENDIX: PERMISSIBLE RANGES FOR m, n FOR THE APPLICATION OF THE SUBHARMONIC MELNIKOV ANALYSIS

The purpose of this Appendix is to provide a bound on the possible values of m, n for which the system (2) can exhibit an m/n resonance (10), for a fixed value of the energy, h. The condition for the existence of a resonant torus in the uncoupled system (9) (corresponding to $\varepsilon = 0$) is given by expression (11):

$$\frac{nK(k_1)}{H_1^{1/4}} = \frac{mK(k_2)}{H_2^{1/4}} \quad \text{(resonance condition)}. \tag{11}$$

Taking into account the fact that the total energy of the unperturbed motion is the sum of the energies of the uncoupled oscillators 1 and 2, i.e. that $h = h_1 + h_2$, the resonance condition (11) becomes

$$\frac{nK\left[\dfrac{(H_1^{1/2}-1)^{1/2}}{2^{1/2}H_1^{1/4}}\right]}{H_1^{1/4}} = \frac{mK\left[\dfrac{(\bar{H}_1^{1/2}-1)^{1/2}}{2^{1/2}\bar{H}_1^{1/4}}\right]}{\bar{H}_1^{1/4}} \tag{A1}$$

where

$$H_1 = 1 + 4h_1, \qquad \bar{H}_1 = 1 + 4(h - h_1).$$

It will be shown that for fixed h, and for m and n in a certain range, equation (A1) gives a unique solution for h_1. This implies that the unperturbed oscillator has a dense set of resonant tori in any neighborhood of the orbit $\mathbf{q} = (0, q_2(t)), \mathbf{p} = (0, p_2(t))$ at every energy level h [11]. Equation (A1) can be regarded as a transcendental equation in h_1. To show uniqueness of solutions for h_1, the monotonicity of the following quantity is examined:

$$D(u) \equiv K\left\{\frac{[(1+4u)^{1/2}-1]^{1/2}}{2^{1/2}(1+4u)^{1/4}}\right\} \Big/ (1+4u)^{1/4}, \quad u \in [0, h). \tag{A2}$$

It can be easily shown that $D(u)$ is a monotonically decreasing function of u in the domain $u \in [0, h)$. Thus, the left-hand side of equation (A1) is monotonically decreasing, whereas the right-hand side is monotonically increasing for $h_1 \in [0, h)$. Therefore, equation (A1) is guaranteed to have a unique solution for h_1, when the

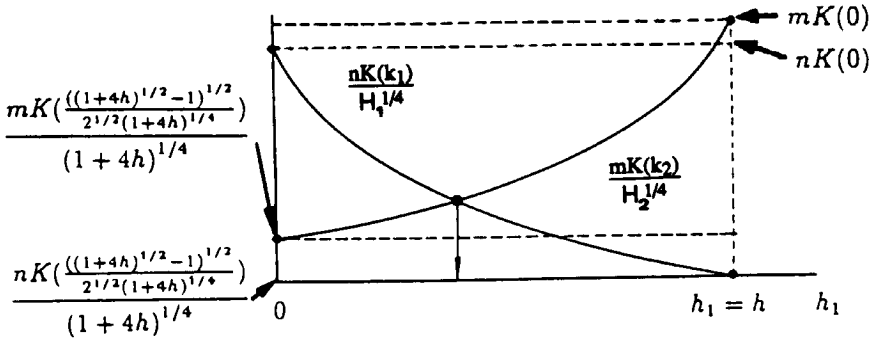

Fig. A1. Graphical solution for h_1 of equation (A1)

following inequalities are satisfied (see Fig. A1):

$$mK\left\{\frac{[(1+4h)^{1/2}-1]^{1/2}}{2^{1/2}(1+4h)^{1/4}}\right\}\Big/(1+4h)^{1/4} \leq nK(0)$$

$$nK\left\{\frac{[(1+4h)^{1/2}-1]^{1/2}}{2^{1/2}(1+4h)^{1/4}}\right\}\Big/(1+4h)^{1/4} \leq mK(0). \tag{A3}$$

The inequalities (A3) pose certain restrictions on the values of m and n. For example, for $h = 1$ the ratio m/n must be in the range $0.72411 \leq m/n \leq 1.38100$, whereas for $h = 50$ it must be satisfied that $0.3087 \leq m/n \leq 3.2395$. Note that as the total energy of the free motion increases, the "permissible" range of values of the ratio m/n also increases.

If the value of m/n is out of the aforementioned range, equation (A1) may not have a unique solution for h_1 in $[0, h)$, and the perturbation analysis is not justified.